Reactions of Laser-Ablated Platinum with Nitrogen: Matrix Infrared Spectra of Platinum Nitride, Complexes, and Anions

Angelo Citra, Xuefeng Wang, William D. Bare, and Lester Andrews*

Department of Chemistry, University of Virginia, Charlottesville, Virginia 22904-4319

Received: April 24, 2001; In Final Form: June 11, 2001

Several new platinum nitride species are produced by the reaction of laser-ablated platinum with pure nitrogen, and their frequencies calculated by density functional theory in addition to the complexes observed in earlier thermal atom studies. Platinum forms PtN and a number of molecules derived from PtN including NNPtN, PtPtN, Pt_2N, and PtNNPt, and PtNNN from reaction with N_3 radical in pure nitrogen. The PtNN complex is characterized by the Pt−N stretching mode at 499.6 cm^{-1} and its combination band at 2669.6 cm^{-1} with the strong N−N fundamental at 2168.5 cm^{-1} in solid argon. Absorptions are observed for Pt_xNN, $PtNN^-$, $Pt(NN)_2^-$, and $Pt(NN)_2$ in solid argon and neon.

Introduction

The interaction between platinum and dinitrogen is important in catalytic processes involving nitrogen fixation.[1] However, given enough energy, chemical reactions can occur. Reactions of third-row transition metal atoms with nitrogen have been investigated in this laboratory using the methods of laser ablation, matrix isolation, and infrared spectroscopy.[2−6] In this paper we report the formation of platinum nitride and compare it to the nitrides of other metals. In particular, the diatomic molecules MN are discussed in detail as gas-phase data are also available in some cases, including PtN.[7] Assignments are supported by density functional theory (DFT) calculations recently applied successfully to platinum hydrides[8] and found to be of similar accuracy to high level ab initio calculations for PtN.[9,10]

The spectra of Ni, Pd, and Pt complexes with dinitrogen were investigated nearly 30 years ago using thermal[11,12] and discharge sputtering[13] atom sources, but only recently has the far-infrared spectrum been observed for dilute samples and all modes assigned for NiNN.[14] Our laser-ablation investigation provides a large yield of PtNN, and we also report the perhaps surprisingly high 499.6 cm^{-1} Pt−NN stretching frequency in the complex and detection of the corresponding anion $PtNN^-$ from electron capture.

Methods

The experiment for laser ablation and matrix isolation has been described in detail previously.[15,16] Briefly, the Nd:YAG laser fundamental (1064 nm, 10 Hz repetition rate, 10 ns pulse width, 5−50 mJ/pulse) was focused on a rotating platinum metal target (crucible). Laser-ablated platinum was co-deposited with nitrogen gas ($^{14}N_2$, $^{15}N_2$, $^{14}N_2 + {}^{15}N_2$) onto a 7−8 K CsI window at 2−4 mmol/h for 30 min to 1 h. Complementary experiments were done with dilute N_2 in argon and in neon on a 5 K window. Infrared spectra were recorded at 0.5 cm^{-1} resolution on a Nicolet 750 spectrometer with 0.1 cm^{-1} accuracy using a HgCdTe detector. Matrix samples were annealed at a range of temperatures and subjected to broadband irradiation by a medium-pressure mercury arc (Philips, 175 W) with the globe removed ($\lambda > 240$ nm).

Density functional theory calculations were performed on platinum nitrides and complexes using the Gaussian 94 program.[17] Since vibrational frequencies are most important for this work, the BPW91 functional was used in all calculations, with the B3LYP functional employed for comparison in selected cases.[18−20] The 6-311+G(d) basis set was used to represent nitrogen,[21] and the LanL2DZ effective-core potential for platinum.[22,23]

Results and Discussion

Absorptions due to platinum nitride, platinum dinitrogen complex species, and the results of supporting DFT calculations will be described in turn for nitrogen (Table 1), argon (Table 2), and neon (Table 3) matrix investigations.

PtN, NNPtN, and PtNNN in Solid Nitrogen. A sharp band is observed at 893.1 cm^{-1} in pure nitrogen with a ^{15}N counterpart at 865.2 cm^{-1} and no intermediate bands in the mixed $^{14}N_2 + {}^{15}N_2$ isotopic experiment. The nitrogen 14/15 isotopic ratio of 1.0323 is very close to the harmonic PtN diatomic value of 1.0325, and the 893.1 cm^{-1} band can be assigned to PtN as it is just below the 937.0 cm^{-1} frequency for PtN in the gas phase, based on $\omega_e = 947.0$ cm^{-1} and $\omega_e x_e = 5.0$ cm^{-1} for the $^2\Pi$ ground state.[7] The interactions between PtN and the nitrogen matrix are substantial, as shown by the sizable matrix shift. This band is almost completely destroyed on annealing and is replaced by another sharp band at 854.7 cm^{-1} with associated sharp absorptions at 2280.0 and 2272.2 cm^{-1}. This 854.7 cm^{-1} band also has an isotopic ratio of 1.0323 and is assigned to the Pt−N stretch of NNPtN where one nitrogen molecule complexes PtN. The latter bands have a higher 14/15 ratio, 1.0345, close to that for N_2 itself, 1.0348, and are assigned to the perturbed N−N stretching mode in the NNPtN complex. The new mixed isotopic bands suggest slight coupling between NN and PtN in this complex. When the matrix is irradiated with UV/visible light ($\lambda > 380$ nm is sufficient) the new bands are completely destroyed and the 893.1 cm^{-1} band reappears showing that the complexation is completely reversible (Figures 1 and 2).

10.1021/jp011542l CCC: $20.00
Published on Web 08/01/2001

TABLE 1: Infrared Absorptions (cm^{-1}) from Laser-Ablated Platinum Atoms Co-deposited with Pure Nitrogen at 7−8 K

$^{14}N_2$	$^{15}N_2$	$^{14}N_2 + {}^{15}N_2$	$^{14}N_2/{}^{15}N_2$ ratio	assignment
2663.7	2577.2	2663.7, 2577.2, 2642, 2598	1.0336	$Pt(NN)_2$
2328.0	2249.8	2328.0, 2249.8	1.0348	N_2 perturbed
2280.0	2204.0	2280.0, 2278.4	1.0345	NNPtN
2272.2	2196.4	2272.2, 2198.0	1.0345	N
				NPtN
2261.8	2186.5	2261.7, 2189.1	1.0344	$Pt_x(NN)_y$
2241.7	2167.1		1.0344	$Pt_x(NN)_y$
2238.1	2163.5	2178	1.0345	$Pt_x(NN)_y$
2210.0[a]	2136.5[a]		1.0344	$(Pt(NN)_2^+)$
2205.7	2132.2	2234.2, 2205.7, 2146.2, 2132.2	1.0345	$Pt(NN)_2$
2203.8[c]	2130.4[c]	2240.3, 2203.8, 2151.8, 2130.4	1.0345	$Pt(NN)_2$ (site)
2198.0	2125.1	2198.0, 2125.1	1.0343	Pt_xNN
2173.0	2100.6	2173.0, 2100.6	1.0346	PtNN
2133.0	2061.6	2061.7	1.0348	Pt_xNN
2104.4[b]	2035.0[b]	2080.7, 2051.3, 2039.7, 2035.0	1.0341	PtNNN
2101.2	2031.8		1.0342	PtNNN site
2077.8[c]	2009.5[c]		1.0340	N_3^-
2048.9[c]	1980.7[c]	2048.9, 1980.7	1.0344	$PtNN^-$
2003.4	1937.6		1.0340	N_3^-
1862.5	1803.5	too weak	1.0327	$Pt(NN)_2^-$
1657.7	1603.3	1657.7, 1649.4 1613.0, 1603.3	1.0339	N_3
1389.5[b]	1343.4[b]	too weak	1.0343	PtNNN
1386.6	1340.6		1.0343	PtNNN site
1095.2	1059.8	1095.2, 1059.8	1.0334	PtPtN
1028.9	996.0	1028.9, 996.0	1.0330	Pt_3N
1022.6	989.8	1022.6, 989.8	1.0331	Pt_3N (site)
945.1	916.1	945.1, 916.1	1.0317	Pt_x-PtN
911.2	882.8	911.2, 882.8	1.0322	Pt_x-PtN
910.2	881.8	910.2, 881.8	1.0322	Pt_x-PtN
908.9	880.5	908.9, 880.5	1.0323	Pt_x-PtN
897.8	869.6	897.8, 869.6	1.0324	Pt_x-PtN
893.1	865.2	893.1, 865.2	1.0323	PtN
854.7	828.0	854.7, 828.0	1.0323	NNPtN
732.1	709.2	754.6, 732.1, 709.2	1.0323	Pt_2N
722.1	698.9	722.1, 710.6, 698.9	1.0332	PtNNPt (site)
713.8	690.9	713.8, 702.5, 690.9	1.0332	PtNNPt

[a] Absorptions observed only with CCl_4 added to nitrogen. [b] Bands enhanced 10-fold with lower laser power and 5 K substrate. [c] Bands decreased 10-fold with CCl_4 added to nitrogen.

Both the BPW91 and B3LYP functionals (Tables 4 and 5) predict a $^2\Pi$ ground state for PtN and frequencies of 975.2 and 975.8 cm^{-1}, respectively, in reasonable agreement with the gas phase (937.0 cm^{-1})[7] and nitrogen matrix (893.1 cm^{-1}) values but higher than the MRSDCI value (844 cm^{-1}).[9] The frequencies of the nitrogen complex NNPtN have also been calculated, and the PtN stretching frequency is decreased about 80 cm^{-1} relative to that in isolated PtN, close to the observed shift. The lower frequency and longer PtN bond indicates that the bonding is weakened when the PtN molecule binds to N_2. On the other hand the N−N frequency at 2280.0 cm^{-1} is above the PtNN value (2173.0 cm^{-1}), suggesting that the PtN interaction with N_2 is weaker than the Pt atom interaction with N_2. The dinitrogen stretching mode of NNPtN is 10 times as intense as the PtN stretching mode, far less than the DFT intensity ratios 75:1 (BPW91) and 146:1 (B3LYP), which are in only qualitative agreement. Finally, the exothermic energy change upon complexation of PtN by N_2, calculated to be −37 kJ/mol (BPW91) or −32 kJ/mol (B3LYP), is in agreement with the observation of spontaneous reaction during annealing.

Since PtN is not prepared in thermal Pt atom experiments with N_2, PtN must be formed here by the direct Pt + N atom reaction, which is calculated to be exothermic (390 kJ/mol, BPW91; 307 kJ/mol, B3LYP). The DFT energies are higher than FOCI (254 kJ/mol) and MRSDCI (238 kJ/mol) values.[9] The production of N atoms in these experiments is attested by the presence of strong N_3 radical absorption at 1657.7 cm^{-1}.[16,24] The failure to observe NNPtN on deposition where excess N_2 is present may be due to the highly exothermic nature of reaction

TABLE 2: Infrared Absorptions (cm^{-1}) from Laser-Ablated Platinum Atoms Co-deposited with 2% N_2 in Argon at 7−8 K

$^{14}N_2$	$^{15}N_2$	$^{14}N_2/{}^{15}N_2$ ratio	$^{14}N_2 + {}^{14}N^{15}N + {}^{15}N_2$[a]	assignment
2669.6[b]	2582.6[b]	1.0337	2627.6, 2624.9	PtNN
2646.6	2560.3	1.0337		$Pt(NN)_2$
2550.7	2466.4	1.0342	2511, −	$(PtNN^-)$
2242.6	2167.1	1.0348		$Pt_x(NN)_y$
2233.2[c]	2158.4[c]	1.0347		$Pt_x(NN)_y$
2230.3[d]	2155.7[d]	1.0346		$((NN)_2^+)$
2218.2	2143.8	1.0347		$Pt_x(NN)_y$
2200.9	2127.6	1.0345		$Pt(NN)_2$ site
2195.4[e]	2122.2[e]	1.0345	2159.0[f]	$Pt(NN)_2$
2172.6	2100.3	1.0344		PtNN site
2168.5	2096.2	1.0345	2134.4, 2131.0	PtNN
2132.3	2061.5	1.0343		Pt_2NN
2128.8	2058.4	1.0342	2095.2, 2092.4	Pt_xNN
2051.5	1983.2	1.0344		$PtNN^-$ site
2045.8	1977.6	1.0344	2014.3, 2010.3	$PtNN^-$
672.1	651.2	1.0321	661.2	(PtNNPt)[g]
506.1	491.6	1.0295		PtNN site
499.6	484.9	1.0303	492.2	PtNN
491.9	478.0	1.0291		Pt_2NN
490.9	476.2	1.0309	483.2	Pt_xNN

[a] New bands observed in addition to $^{14}N_2$ and $^{15}N_2$ counterparts. [b] No new bands with $^{14}N_2 + {}^{15}N_2$ sample unless otherwise noted. [c] With $^{14}N_2 + {}^{15}N_2$ sample, 2226 and 2164 cm^{-1} bands observed. [d] Bands observed only on annealing with CCl_4 added to nitrogen. [e] With $^{14}N_2 + {}^{15}N_2$ sample, the 2195.4 and 2122.2 cm^{-1} bands were observed along with new features at 2228.3 and 2139.1 cm^{-1}. [f] Other mixed isotopic bands are masked (see Figure 7). [g] Tentative counterpart of neon matrix absorption.

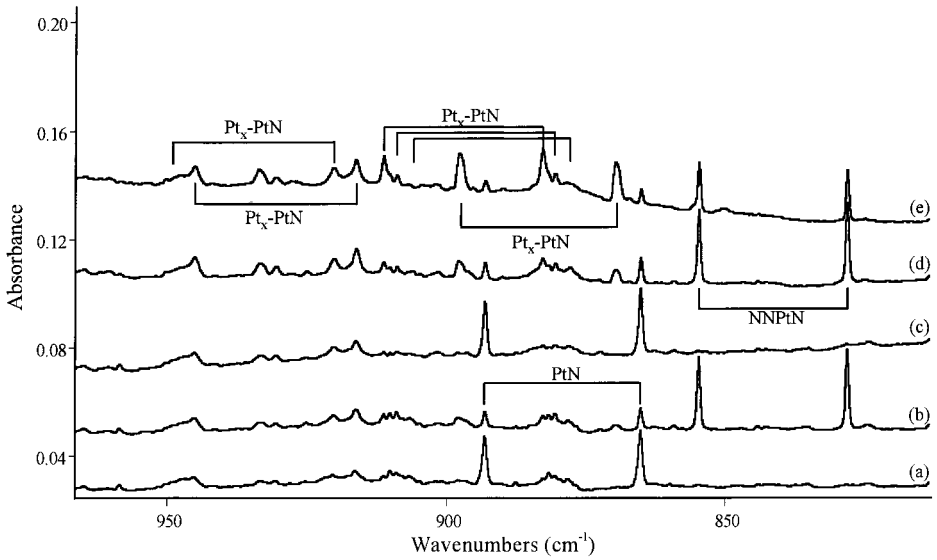

Figure 1. Infrared spectra in the 950−800 cm^{-1} region for laser-ablated platinum atoms after (a) 60 min deposition with $^{14}N_2 + {}^{15}N_2$, (b) annealing to 25 K, (c) UV/Vis irradiation, (d) annealing to 30 K, and (e) annealing to 38 K.

TABLE 3: Infrared Absorptions (cm^{-1}) from Laser-Ablated Platinum Atoms Co-deposited with 2% N_2 in Neon at 5 K

$^{14}N_2$	$^{15}N_2$	$^{14}N_2/^{15}N_2$ ratio	$^{14}N_2 + {}^{15}N_2$[a]	assignment
2660.0	2573.4	1.0337	2683, 2634, 2596	$Pt(NN)_2$
2328.2	2250.2	1.0347		$(N_2)_x$
2238.7	2164.0	1.0345		$Pt_x(NN)_y$
2237.4	2163.1	1.0344	2259.0, 2178.8	$(NN)_2^+$
2223.8	2149.6	1.0345		$Pt_x(NN)_y$
2212.1				$(Pt(NN)_2^+)$
2208.1	2134.4	1.0345		$Pt(NN)_2$ site
2206.9	2133.4	1.0345	2238, 2150	$Pt(NN)_2$
2173.9	2101.4	1.0345		PtNN site
2169.5	2097.5	1.0343		PtNN
2140.9	2140.9			CO (impurity)
2090.4	2021.1	1.0343		Pt_xNN?
2054.1	1986.1	1.0342		$PtNN^-$
2016.7	1949.2	1.0346		(Pt_xNN^-)
1869.0	1810.0	1.0326	1903, 1833	$Pt(NN)_2^-$
1648.0	1594.0	1.0339		N_3
722.0	698.9	1.0331	710.3	PtNNPt site
716.8	693.9	1.0330	705.3	PtNNPt

[a] New bands observed in addition to $^{14}N_2$ and $^{15}N_2$ counterparts.

1; annealing is required to allow the proper reagent approach for reaction 2.

$$Pt + N \rightarrow PtN(^2\Pi)\Delta E = -390 \text{ kJ/mol} \quad (1)$$

$$N_2 + PtN \rightarrow NNPtN(^2A'')\Delta E = -37 \text{ kJ/mol} \quad (2)$$

Another set of sharp bands grows on annealing at 2104.2, 2101.2 cm^{-1} (Figure 2), and 1389.5 cm^{-1} (not shown). These bands are 80% destroyed by broadband irradiation but are regenerated together on further annealing. A final irradiation completely destroys NNPtN but again removes only 80% of the 2104.4 and 1389.5 cm^{-1} bands. In the $^{15}N_2$ experiment, $\lambda > 380$ nm light completely destroys NNPtN with no effect on the latter bands. The 14/15 ratios, 1.0341 and 1.0343, point to pure N−N stretching modes and the regions are reminiscent of metal azide species,[25,26] which can be formed by the metal reaction with N_3 radical. The antisymmetric N−N−N vibration in MNNN is expected to give a sextet of bands in the $^{14}N_2 + {}^{15}N_2$ experiment: only four of these are observed owing to masking by stronger absorptions near 2100 cm^{-1}. DFT calculations predict a stable trans bent PtNNN molecule slightly higher in energy than NNPtN (+66 kJ/mol, BPW91; +77 kJ/mol, B3LYP) with strong IR bands at 2080.1 and 1198.7 cm^{-1} (B3LYP) and 4:1 relative intensity, which are in good agreement with the 2104.4 and 1389.5 cm^{-1} bands with 5:1 relative intensity. Both BPW91 and B3LYP functionals predict the symmetric N−N−N stretch too low: this discrepancy may arise from a difference in structure between the calculated and matrix-isolated molecules.

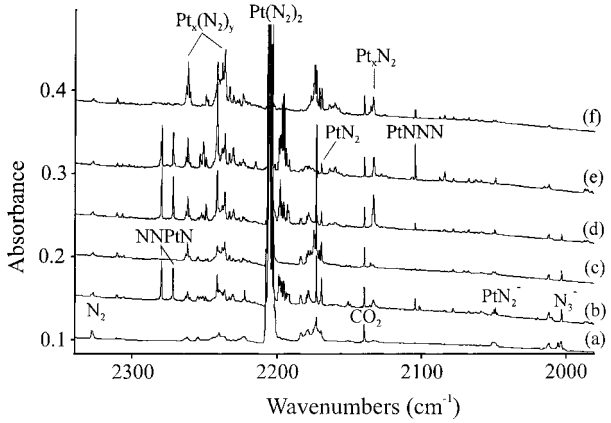

Figure 2. Infrared spectra in the 2340−1980 cm^{-1} region for laser-ablated platinum atoms after (a) 30 min deposition with $^{14}N_2$, (b) annealing to 25 K, (c) UV/Vis irradiation, (d) annealing to 30 K, (e) annealing to 35 K, and (f) another irradiation with UV/vis.

Similar MNNN azide molecules have been observed for Al, Ga, In, and Tl,[25,26] and the PtNNN spectrum most closely resembles that for the less ionic Al species, which is calculated to have a linear structure. It was suggested from isotopic data that these molecules were formed by the metal atom reaction with N_3 radical. In the case of platinum, the greater stability for NNPtN favors a like mechanism, and reaction 3 is exothermic by 263 kJ/mol (BPW91). Even though the NNPtN isomer is more stable energy wise, once formed, PtNNN is kinetically stable in the matrix. Note, however, that NNPtN is more photosensitive than PtNNN (Figure 2).

$$Pt + N_3 \rightarrow PtNNN(^2A'')\ \Delta E = -263 \text{ kJ/mol} \quad (3)$$

Other PtN Species in Solid Nitrogen. A series of bands observed in the 950−900 cm^{-1} region shows doublets in the

TABLE 4: Geometries, Frequencies, and Energies of Platinum Nitride Products Calculated with the BPW91 Functional

molecule	electronic state (point group)	relative energy (kJ/mol)	geometry (Å, deg)	frequencies (cm^{-1}) [intensities] [km/mol]
NN	$^1\Sigma^+$ ($D_{\infty h}$)		NN: 1.107	2349.3 [0]
PtN	$^2\Pi$ ($C_{\infty v}$)	0	PtN: 1.703	975.2 [8]
PtNN	$^1\Sigma^+$ ($C_{\infty v}$)	0	PtN: 1.817 NN: 1.130 ∠PtNN: 180.0	2162.5 [250], 531.3 [8], 336.5 [4 × 2][a]
$Pt(N_2)$	$^1A_1$ (C_{2v})	+101	PtN: 2077 NN: 1.164	1891.8 [99], 397.2 [10], 214.7 [3]
$PtNN^+$	$^2\Sigma^+$ ($C_{\infty v}$)	+900	PtN: 1.902 NN: 1.116 ∠PtNN: 180.0	2255.3 [21], 430.6 [11], 328.2 [2] × 2
	$^4\Delta$ ($C_{\infty v}$)	+1092	PtN: 2.331 NN: 1.106 ∠PtNN: 180.0	2346.0 [44], 336.9 [0] × 2, 173.8 [5]
$PtNN^-$	$^2A'$ (C_s)	−139	PtN: 1.884 NN: 1.147 ∠PtNN: 168.3	2028.6 [644], 455.2 [6], 132.7 [45]
	^{4}?	+119	PtN: 2.036 NN: 1.160 ∠PtNN: 180.0	1843.2 [1673], 308.0 [31 × 2], 129.3 [6]
$NNPtN_t$	$^2A''$ (C_s)	0	PtN_t: 1.741 PtN: 2.069 NN: 1.118 $\angle N_tPtN$: 151.4 ∠PtNN: 171.4	2201.9 [298], 889.0 [4], 310.5 [4], 287.9 [0], 273.0 [2], 94.1 [4]
	$^4\Sigma^-$ ($C_{\infty v}$)	+19	PtN_t: 1.793 PtN: 2.030 NN: 1.121 $\angle N_tPtN$: 180.0 ∠PtNN: 180.0	2182.4 [451], 736.9 [10], 364.5 [0], 336.8 [16], 290.4 [2], 98.8 [3]
PtNNN	$^2A''$ (C_s)	+66	PtN: 1.876 NN: 1.254 NN: 1.155 ∠PtNN: 119.0 ∠NNN: 167.0	1993.3 [383], 1130.2 [51], 694.0 [7], 457.2 [4], 414.4 [1], 167.3 [5]
Pt_2N	$^2B_2$ (C_{2v})	0	PtPt: 2.757 PtN: 1.813 ∠PtNPt: 99.0	737.8 [29], 723.0 [11], 129.0 [1]
	$^4A_1$ (C_{2v})	+95	PtPt: 2.596 PtN: 1.907 ∠PtNPt: 85.8	650.2 [12], 476.3 [0], 129.1 [1]
PtPtN	$^2A'$ (C_s)	+89	PtPt: 2.368 PtN: 1.702 ∠PtPtN: 167.4	999.7 [64], 224.3 [1], 45.8 [1]
	$^4A''$ (C_s)	+158	PtPt: 2.467 PtN: 1.754 ∠PtPtN: 118.2	823.6 [6], 184.2 [0], 125.2 [2]
PtPtNN	$^1\Sigma$ ($C_{\infty h}$)	0	PtPt: 2.421 PtN: 1.921 NN: 1.127	2157.9 [611], 419.2 [28], 372.7 [5 × 2], 202.5 [0.1], 40.0 [1 × 2]
$(Pt_2)(N_2)$	$^1A_1$ (C_{2v})	+25	PtPt: 2.613 PtN: 1.957 NN: 1.198 ϕ(NPtPtN): 0.0	1645.0 [205], 577.9 [12], 514.0 [6], 358.4 [0] ... 155.0 [0]
	$^3A_2$ (C_{2v})	+97	PtPt: 2.471 PtN: 2.308 NN: 1.147 ϕ(NPtPtN): 0.0	1970.0 [210], 384.8 [2], 242.0 [0] ... −44.5 [4]
PtNNPt	$^1\Sigma_g^+$ ($D_{\infty h}$)	+59	Pt: 1.824 NN: 1.148	2112.2 [0], 713.7 [81], 282.2 [0 × 2], 184.1 [0], 102.5 [8 × 2]
$(PtN)_2$	^1A_g (C_{2h})	+337	PtN: 1.922 PtPt: 2.862 ∠NPtPt: 96.2 ϕ(NPtPtN): 180.0	704.6 [0], 571.8 [9], 472.5 [39], 463.6 [0], 234.1 [13], 174.7 [0]
	$^3B_1$ (C_{2v})	+329	PtN: 1.942 PtPt: 2.925 ∠PtNPt: 97.7 ϕ(NPtPtN): 158.7	669.2 [2], 582.6 [25], 503.9 [18], 430.7 [0], 188.7 [1], 97.4 12]
NPtPtN	^1A_g (C_{2h})	+446	PtN: 1.719 PtPt: 2.513 ∠NPtPt: 121.9 ϕ(NPtPtN): 180.0	941.3 [0], 920.1 [112], 184.8 [0] ... 71.9 [7]

TABLE 4 (Continued)

molecule	electronic state (point group)	relative energy (kJ/mol)	geometry (Å, deg)	frequencies (cm^{-1}) [intensities] [km/mol]
NPtPtN	^3A_u (C_{2h})	+365	PtN: 1.728 PtPt: 2.496 ∠NPtPt: 129.3 ϕ(NPtPtN): 180.0	906.8 [0], 830.6 [135], 190.6 [0] ... 65.3 [8]
$PtPtN_2$	$^3B_1$ (C_{2v})	+460	PtPt: 2.482 PtN: 1.747 ∠PtPtN: 117.2	928.9 [0], 825.0 [58], 282.7 [2], 182.2 [1], 151.7 [3], 63.2 [1]
$Pt(NN)_2$	$^1\Sigma_g^+$ ($D_{\infty h}$)	0 (−155)[c]	PtN: 1.904 NN: 1.121 ∠PtNN: 180.0	2240.0 [0], 2190.4 [919], 470.0 [0], 431.9 [102] ... 67.0 [0][b]
$Pt(NN)_3$	$^1A_1''$ (D_{3h})	(+54)[d]	PtN: 2.006 NN: 1.121 ∠PtNN: 180.0 ∠NPtN: 120.0	2218.0, 2183.7 [637 × 2], 417.2 [0], 372.4 [1] ... 26.5 [2 × 2]
$Pt(NN)_2^+$	$^2\Sigma_g^+$ ($D_{\infty h}$)	+894[e]	PtN: 1.961 NN: 1.112 ∠PtNN: 180.0	2304.1 [0], 2278.5 [78], 464.2 [0 × 2], 413.8 [0], 397.8 [30] ... 94.4 [11 × 2]
$Pt(NN)_2^-$	$^2\Sigma_g^+$ ($D_{\infty h}$)	−78[e]	PtN: 1.891 NN: 1.157 ∠PtNN: 180.0	2012.9 [0], 1928.4 [2469], 485.8 [0], 432.8 [13] ... 86.5 [4 × 2]

[a] Isotopic frequencies: Pt-14−15: 2128.8, 522.4, 333.4 cm^{-1}; Pt-15−14: 2123.8, 523.7, 328.3 cm^{-1}; Pt-15−15: 2089.4, 515.4, 325.2 cm^{-1}. [b] Dinitrogen stretching modes: 2222.5 [215], 2133.1 [674] for 14−14, 15−15 isotope and 2164.3 [0], 2116.3 [858] for $(15-15)_2$ isotope. [c] Relative to PtNN + N_2. [d] Relative to $Pt(NN)_2$ + N_2. [e] Relative to $Pt(NN)_2$.

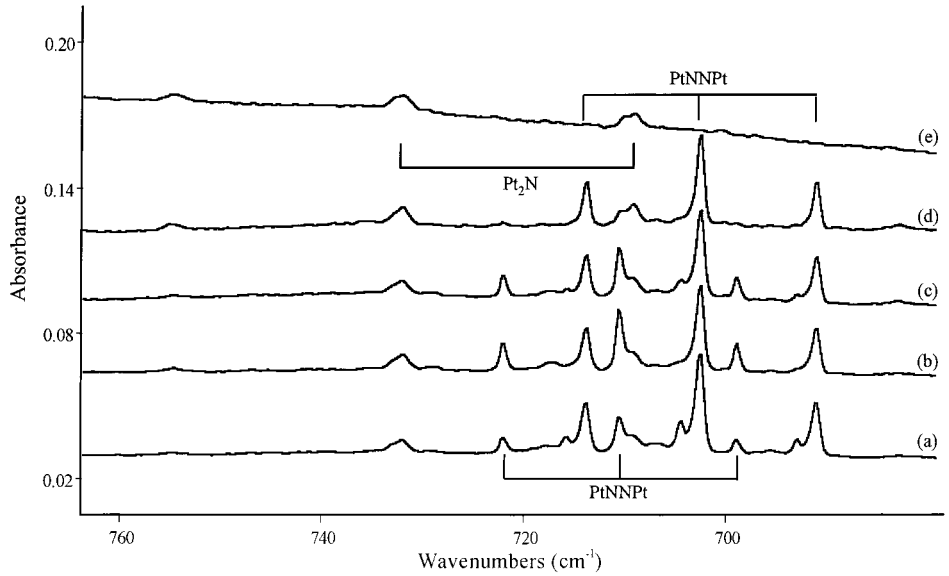

Figure 3. Infrared spectra in the 760−680 cm^{-1} region for laser-ablated platinum atoms after (a) 60 min deposition with $^{14}N_2$ + $^{15}N_2$, (b) annealing to 25 K, (c) UV/Vis irradiation, (d) annealing to 30 K, (e) annealing to 38 K.

mixed isotopic experiment and isotopic ratios in the range 1.0317−1.0324, which are slightly below the diatomic value (Figure 1). The bands are broader than those due to PtN or NPtNN and are less intense. They are present initially, grow during annealing, decrease on irradiation with ultraviolet/visible light, and are due to perturbed PtN species. The range of ratios and the blue shifts in some of these bands suggest that these are not simply dinitrogen complexes of PtN. Their exact nature cannot be determined, but it is likely that the bands are due to PtN perturbed by small platinum clusters, but such assignments are tentative.

A sharp band is observed at 713.8 cm^{-1}, with a weaker matrix site at 722.1 cm^{-1}. The $^{15}N_2$ counterpart bands are observed at 690.9 and 698.9 cm^{-1} and give isotopic ratios of 1.0331 and 1.0332, respectively. This band is unique in the nitride region in that intermediate bands observed at 702.5 and 710.6 cm^{-1} in the $^{14}N_2$ + $^{15}N_2$ mixed isotopic experiment form 1:2:1 intensity patterns (Figure 3). Experiments with 2% N_2 in neon gave an analogous band at 716.8 cm^{-1} and a mixed isotopic triplet absorption pattern. This indicates that two nitrogen molecules are involved in the creation of this product. The most obvious assignment is to a dimer of PtN, since the molecule is abundant in the nitrogen matrix and the nitrogen atoms come from two different N_2 molecules and two platinum atoms are implicated. Several PtN dimer structures were calculated with DFT, the bridged dimer $(PtN)_2$, and the open NPtPtN and PtNNPt forms with terminal Pt−N bonds. The calculated frequencies for $(PtN)_2$ in both singlet and triplet states are below 500 cm^{-1}, far too low to account for the observed bands, and the ring structures are high energy species (Table 4). The calculation for NPtPtN in a triplet state with the Pt−N bonds in a trans arrangement is also high energy, but the strong calculated frequency is in the appropriate region. However, the linear PtNNPt dimer is only 59 kJ/mol above the lowest energy structure (PtPtNN) to be

TABLE 5: Geometries, Frequencies, and Energies of Platinum Nitride Products Calculated with the B3LYP Functional

molecule	electronic state (point group)	relative energy (kJ/mol)	geometry (Å, deg)	frequencies (cm^{-1}) [intensities] [km/mol]
NN	$^1\Sigma^+$ ($D_{\infty h}$)		NN: 1.096	2444.4 [0]
PtN	$^2\Pi$ ($C_{\infty v}$)		PtN: 1.703	975.8 [11]
PtNN	$^1\Sigma^+$ ($C_{\infty v}$)	0	PtN: 1.849 NN: 1.113 ∠PtNN: 180.0	2278.1 [309], 485.3 [13], 325.1 [3 × 2]
$PtNN^+$	$^2\Sigma^+$ ($C_{\infty v}$)	+871	PtN: 1.963 NN: 1.099 ∠PtNN: 180.0	2397.0 [9], 366.9 [7], 305.3 [1 × 2]
$PtNN^-$	$^2A'$ (C_s)	−309	PtN: 1.883 NN: 1.145 ∠PtNN: 178.9	2343.0 [543], 451.2 [4], −97.5 [28]
$NNPtN_t$	$^2A''$ (C_s)		PtN_t: 1.736 PtN: 2.165 NN: 1.099 ∠N_tPtN: 165.9 ∠PtNN: 176.2	2370.2 [146], 899.0 [1], 266.8 [1], 263.1 [0] ... 45.3 [4]
PtNNN	$^2A''$ (C_s)	+77	PtN: 1.895 NN: 1.241 NN: 1.138 ∠PtNN: 119.6 ∠NNN: 169.8	2080.1 [476], 1198.7 [123], 699.4 [9], 495.2 [5], 442.1 [10], 158.1 [4]
Pt_2N	$^2B_2$ (C_{2v})	0	PtPt: 2.762 PtN: 1.811 ∠PtNPt: 99.4	740.8 [35], 725.1 [3], 129.1 [1]
PtPtN	$^2A'$ (C_s)	+104	PtPt: 2.414 PtN: 1.719 ∠PtPtN: 136.4	817.8 [41], 199.4 [0], 70.4 [3]
$(Pt_2)(N_2)$	$^1A_1$ (C_{2v})	0	PtPt: 2.636 PtN: 1.972 NN: 1.177 ϕ(NPtPtN): 180.0	1766.1 [248], 574.3 [8], 488.9 [7], 356.9 [0] ... 149.4 [0]
$Pt(NN)_2$	$^1\Sigma^+$ ($D_{\infty h}$)	0 (−142)[a]	PtN: 1.922 NN: 1.106 ∠PtNN: 180.0	2349.0 [0], 2306.7 [904], 445.7 [0], 409.8 [113] ... 75.1 [0]
$Pt(NN)_2^+$	$^2\Sigma_g^+$ ($D_{\infty h}$)	+866	PtN: 1.992 NN: 1.098 ∠PtNN: 180.0	2426.4 [0], 2412.0 [35], 441.2 [0] × 2, 380.0 [0], 363.4 [18] ... 91.0 [1 × 2]
$Pt(NN)_3$	$^1A_1$ (C_{2v})	(+66)[b]	PtN: 1.909, 2.193 NN: 1.112, 1.102 ∠PtNN: 180.0, 167.4 ∠NPtN: 88.8, 135.6	2365.1 [123], 2336.8 [260], 2273.3 [659], 446.1 [0], 441.5 [32] ... −154.6 [8]

[a] Relative to PtNN + N_2. [b] Relative to $Pt(NN)_2$ + N_2.

discussed and assigned later, and the strong antisymmetric Pt−N stretching mode computed at 713.7 cm^{-1} is in excellent agreement with experiment. The triplet mixed isotopic absorption spacings, 11.3 and 11.6 cm^{-1} show only slight asymmetry, which is in accord with a symmetric Pt−N stretching mode much lower in frequency, as predicted by calculation. A singlet trapezoidal structure is slightly lower in energy, but the 1645.0 cm^{-1} calculated N−N frequency is not observed.

The 713.8 cm^{-1} absorption is assigned to linear PtNNPt formed by dimerization of PtN. Although the N−N stretching mode is not active, the calculated value, 2112.3 cm^{-1}, is lower than the 2162.5 cm^{-1} frequency calculated for PtNN, to be discussed below.

$$2\ PtN(^2\Pi) \rightarrow PtNNPt\ (^1\Sigma_g^+)\ \Delta E = -496\ kJ/mol \quad (4)$$

Pt_2N Species in Solid Nitrogen. Sharp bands grow in at 1095.2 and 1028.9 cm^{-1} in pure nitrogen during annealing that are not present after deposition (Figure 4). Both bands give doublets in the $^{14}N_2 + {}^{15}N_2$ mixed isotopic experiments, showing that only one nitrogen atom is involved in the mode. The isotopic ratios of 1.0334 and 1.0330 for these bands are very close to the pure nitrogen ratio of 1.0350, which indicates that the nitrogen atom is moving against a large mass. The most logical assignments for these bands are Pt_xN, in which the nitrogen atom moves against a small metal cluster. If the nitrogen atom moves against a mass of Pt_2, and the mode is treated as pseudo diatomic, then the expected isotopic ratio is 1.0337, in close agreement with the observed ratios. The 1095.2 cm^{-1} band has the greatest intensity before the final annealing cycle, while the 1028.9 cm^{-1} band continues to increase at the final annealing. This suggests that the higher frequency band is due to PtPtN, and the lower frequency band is due to a higher cluster, probably Pt_3N.

The DFT calculations for PtPtN predict a doublet ground state and a bent geometry. The two functionals differ somewhat in the description of this molecule; the BPW91 result is closer to a linear geometry and has shorter bond lengths than the B3LYP geometry, partially canceling the tendency for the latter

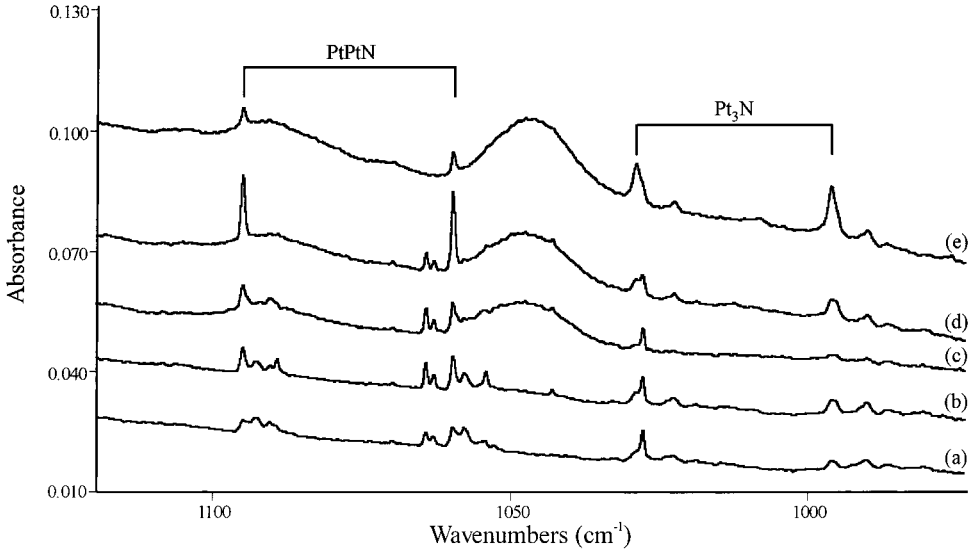

Figure 4. Infrared spectra in the 1120−980 cm^{-1} region for laser-ablated platinum atoms after (a) 60 min deposition with $^{14}N_2 + {}^{15}N_2$, (b) annealing to 25 K, (c) UV/Vis irradiation, (d) annealing to 30 K, (e) annealing to 38 K.

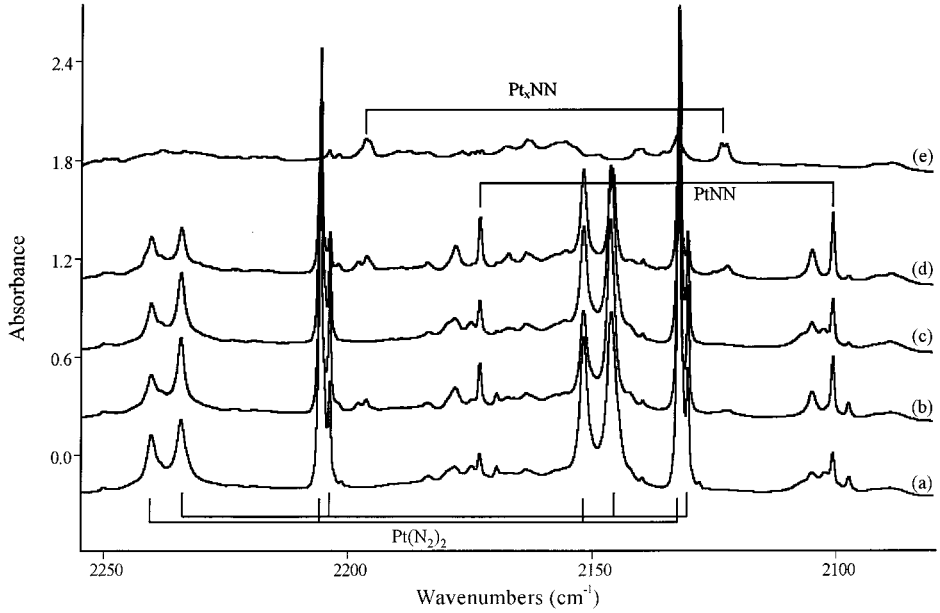

Figure 5. Infrared spectra in the 2250−2080 cm^{-1} region for laser-ablated platinum atoms after (a) 60 min deposition with $^{14}N_2 + {}^{15}N_2$, (b) annealing to 25 K, (c) irradiation with UV/Vis, (d) annealing to 30 K, and (e) annealing to 38 K.

functional to overestimate vibrational frequencies. Both Pt−N stretching modes are in reasonable agreement with the 1095.2 cm^{-1} band and support the assignment.

A new band is observed at 732.1 cm^{-1} on annealing with a $^{15}N_2$ counterpart at 709.2 cm^{-1}. No intermediate band is observed in the mixed isotopic experiment so a single N is indicated, and the isotopic ratio of 1.0323 is very close to that for PtN. However, the band is of considerably lower frequency than that for PtN, and the best assignment is to Pt_2N, where a nitrogen atom bridges across a platinum dimer. This would most likely be formed from addition of a platinum atom to PtN, although the combination of Pt_2 with a nitrogen atom is also possible. If the PtNPt bond angle is 90°, then a diatomic isotopic frequency ratio will result, as is observed. The DFT calculations for Pt_2N support this assignment: the bond angle is 99° with both functionals, close to a right angle, and strong infrared absorptions are predicted at 737.8 cm^{-1} (BPW91) and 740.8 cm^{-1} (B3LYP).

It is interesting that both Pt_2N and PtPtN are observed, despite the greater stability of the former molecule. This indicates that the reactions in the matrix are under kinetic control rather than thermodynamic control. The same was found with the rhodium nitrides, i.e., both RhRhN and Rh_2N were observed in pure nitrogen.[27]

$Pt(NN)_{1,2}$ in Solid Nitrogen. The dinitrogen complex region has been investigated previously[11−13] and the strong 2205.7 cm^{-1} nitrogen matrix band assigned to the possible complexes $Pt(NN)_{1,3}$. However, the work of Green et al. suggests the $Pt(NN)_2$ assignment for the strong nitrogen matrix band.[13] The spectra of Kundig et al.[12a] and our Figure 5 clearly show intermediate mixed isotopic bands, which demonstrate the involvement of more than one NN subunit. For the linear NN−Pt−NN species, both stretching modes are infrared active in the mixed isotopic molecule with intensities depending on the sretch−stretch interaction, as has been shown for linear dicarbonyls.[28−30] The weaker 2173.0 cm^{-1} absorption increases on 25 K annealing then decreases on subsequent annealings; this band could be due to PtNN in matrix environments where another N_2 reagent is not accessible (such as a surface site),

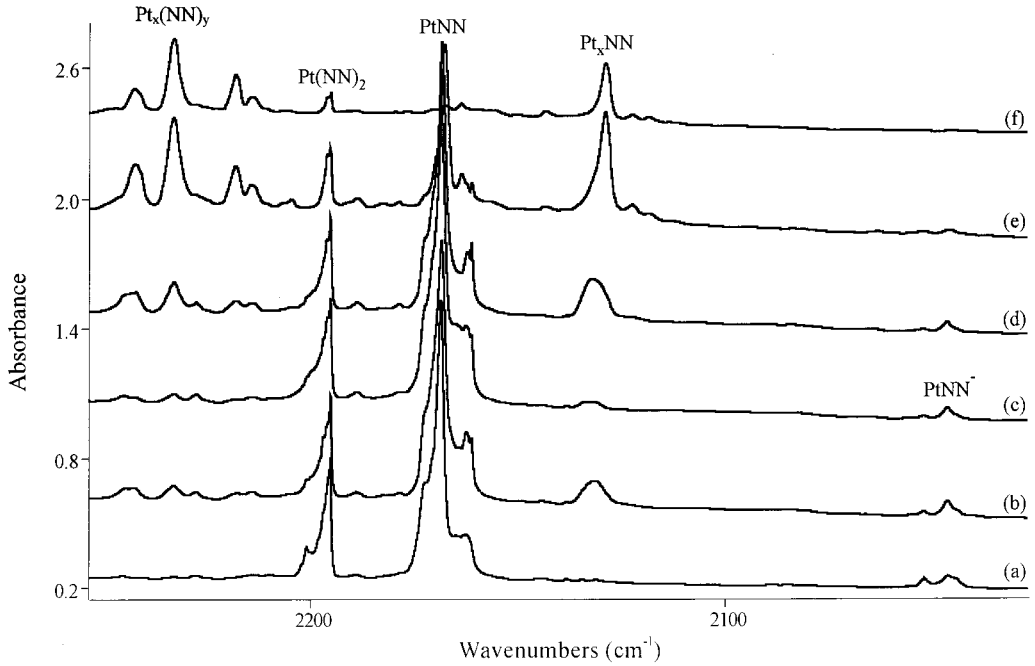

Figure 6. Infrared spectra in the 2250−2030 cm^{-1} region for laser-ablated platinum co-deposited with 2% N_2 in argon at 5 K: after (a) 60 min deposition, (b) 25 K annealing, (c) UV/Vis irradiation, (d) 30 K annealing, (e) 40 K annealing, and (f) 45 K annealing.

but we cannot be certain. The PtNN complex is observed at 2168.5 cm^{-1} in solid argon[12,13] as will be discussed below.

Our DFT calculations for these species lend support to the assignments of the latter groups[12,13] to PtNN and the Argonne workers[13] to Pt(NN)$_2$; the Toronto group agrees in their later paper.[12b] Both functionals show the same prediction for the dinitrogen stretching frequencies: the BPW91 frequencies of 2162.5 and 2190.4 cm^{-1} for PtNN and Pt(NN)$_2$ are within 15 cm^{-1} of the observed values, and the B3LYP frequencies 2278.1 and 2306.7 cm^{-1} require scale factors of 0.954 and 0.956 to match experiment, which is typical for this functional.[31] The extra bands at 2234.2 and 2146.2 cm^{-1} in the mixed $^{14}N_2/^{15}N_2$ experiment (Figure 5) are appropriate for symmetric and antisymmetric N−N modes of the linear $^{15}N^{15}N-Pt-^{14}N^{14}N$ molecule and support the Green et a1.[13] assignment of the nearby argon matrix band to Pt(NN)$_2$. The strong 2205.7 cm^{-1} nitrogen matrix band must be assigned likewise. This disagrees with the earlier assignments[11,12] of the latter band to Pt(NN)$_{1,3}$. Our DFT calculations predict the Pt(14−14)(15−15) isotopic bands 32.1 and 16.8 cm^{-1} above the pure isotopic bands and with relative intensity 1:3, which is in excellent agreement with the observed 28.5 and 14.0 cm^{-1} separations and band absorbances, and strongly supports this reassignment. Finally, DFT calculations find that naked Pt combines exothermically with two NN ligands (−157 and −155 kJ/mol, respectively (BPW91), and −103 and −142 kJ/mol, respectively (B3LYP), but the third attachment is endothermic (+54 kJ/mol (BPW91) and +66 kJ/mol (B3LYP)): this means that Pt(NN)$_3$ is unstable and that the early claim for its identification[12] must be rejected. Note that the 2280 and 2104 cm^{-1} bands due to PtNNN and NNPtN were not reported previously as neither nitrogen atoms nor nitride products were formed in the thermal platinum−nitrogen matrix experiments.[12]

Sharp, weaker absorptions at 2663.7 and 2577.2 cm^{-1} for $^{14}N_2$ and $^{15}N_2$, respectively, track with the strong 2205.7 and 2132.2 cm^{-1} absorptions and are due to combination bands involving σ_g and σ_u stretching modes. Subtracting the latter from the former bands gives 458 and 445 cm^{-1}, respectively, for possible σ_g Pt−N_2 stretching modes, but the 458/445 = 1.0292 ratio is too low (calculated 1.0348) for a σ_g mode, so this combination must be discarded. Subtracting the 2258 cm^{-1} Raman band observed by Kundig et al.[12a] and its calculated $^{15}N_2$ counterpart from the combination bands gives 406 and 395 cm^{-1}, respectively, for possible σ_u Pt−N_2 fundamentals, and the 406/395 = 1.0279 ratio is near that calculated from BPW91 frequencies (1.0269). Hence, the unobserved σ_u Pt−N_2 stretching mode is near 406 cm^{-1}, slightly lower than the BPW91 calculated value (431.9 cm^{-1}, Table 4). In the $^{14}N_2 + {}^{15}N_2$ experiment, four combination bands are possible and several weaker bands are observed: the strongest 2642 cm^{-1} band is probably due to the 2234 cm^{-1} "σ_g" plus a 408 cm^{-1} "σ_u" mode.

Absorptions at 2261.8, 2241.7, 2238.1, 2198.0, and 2133.0 cm^{-1} increased markedly on annealing while the 2205.7 cm^{-1} band decreased. The latter two bands show no evidence of mixed isotopic behavior, but the 2261.8 and 2238.1 cm^{-1} absorptions do reveal new mixed isotopic absorptions. The 2198.0 cm^{-1} band is destroyed by photolysis but returns on further annealing. We believe that the 2198.0 and 2133.0 cm^{-1} absorptions are due to Pt$_x$NN clusters with x probably larger in the 2198.0 cm^{-1} case. The 2261.8, 2241.7, and 2238.1 cm^{-1} bands are probably due to the larger generic clusters noted Pt$_x$(NN)$_y$.

Nitrogen matrix experiments were done on a 5 K substrate with 0.1% CCl_4 added to the nitrogen to serve as an electron trap.[29,32] This reduced the overall band yield (by 70−90%), eliminated the 1862.5 and 2048.9 cm^{-1} bands, reduced by 10× the N_3^- and Pt$_x$(NN)$_y$ aggregate bands, and produced a weak new 2210.0 cm^{-1} absorption. The latter band shifted to 2136.5 cm^{-1} with $^{15}N_2$ giving a 1.0344 ratio. Our DFT calculations find Pt(NN)$_2^+$ to be a $^2\Sigma_g^+$ state with strong absorption blue shifted 88 cm^{-1} from Pt(NN)$_2$. The appearance of a new band with CCl_4 electron trap added is consistent with the cation identification. Hence, the new 2210.0 cm^{-1} absorption is tentatively assigned to Pt(NN)$_2^+$. Argon and neon matrix counterparts of the 2048.9 and 1862.5 cm^{-1} bands will be assigned below to Pt(NN)$_{1,2}^-$, respectively.

Pt(NN)$_{1,2}$ in Solid Argon and Neon. Experiments were performed with 2% N_2 in argon on 5 and 8 K substrates, and representative spectra are shown in Figures 6 and 7. The relative

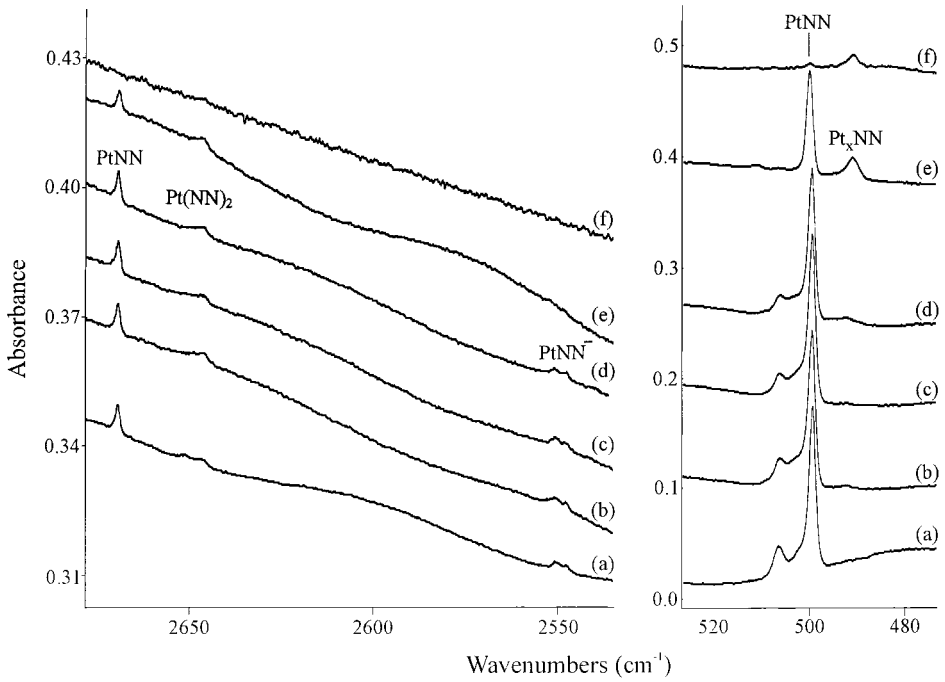

Figure 7. Infrared spectra in the 2680−2530 and 525−475 cm^{-1} regions for laser-ablated platinum co-deposited with 2% N_2 in argon at 5 K: after (a) 60 min deposition, (b) 25 K annealing, (c) UV/Vis irradiation, (d) 30 K annealing, (e) 40 K annealing, and (f) 45 K annealing.

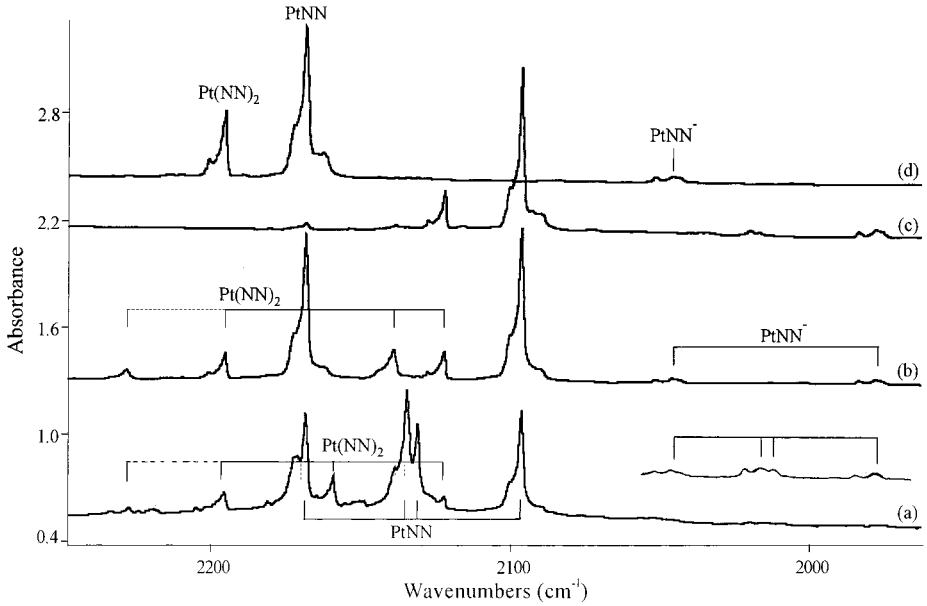

Figure 8. Infrared spectra in the 2250−1960 cm^{-1} region for laser-ablated platinum co-deposited for 60 min with isotopic N_2 in argon. (a) 1% $^{14}N_2$ + 2% $^{14}N^{15}N$ + 1% $^{15}N_2$, (b) 2% $^{14}N_2$ + 2% $^{15}N_2$, (c) 2% $^{15}N_2$, and (d) 2% $^{14}N_2$.

populations of PtNN (2168.5 cm^{-1} in argon) and $Pt(NN)_2$ (2195.4 cm^{-1} in argon) are reversed. The mixed $^{14}N_2$ + $^{15}N_2$ (and $^{14}N_2$ + $^{14}N^{15}N$ + $^{15}N_2$) isotopic data and frequency calculations again support the $Pt(NN)_2$ assignment of Green et al.[13] Both stretching modes are observed for $(^{14}N_2)Pt(^{15}N_2)$ and the strongest new band for $Pt(^{14}N^{15}N)_2$; unfortunately the $Pt(^{14}N_2)(^{14}N^{15}N)$ and $Pt(^{15}N_2)(^{14}N^{15}N)$ bands are masked by $Pt^{14}N^{14}N$ and $Pt^{14}N^{15}N$ absorptions. Likewise, more isotopic information is provided here in support of the earlier assignments[12,13] to PtNN. At lower N_2 concentration, we resolve the PtNN absorption into the expected quartet for two inequivalent nitrogen atoms (Figure 8). In addition, we observe the Pt−NN stretching mode at 499.6 cm^{-1}, with 9% of the intensity of the N−N fundamental in our most dilute experiment (0.2% N_2) where bands are the sharpest. The 499.6 cm^{-1} absorption gives a statistical isotopic triplet because the Pt-14−15 and Pt-15−14 bands (Table 4) are separated by less than the line width (Figure 9). Our BPW91 calculation predicts this band at 531.3 cm^{-1} with 14/15 ratio 1.0308 and 3% of the strongest band intensity, in very good agreement with the observed values. This assignment to the Pt−NN stretching mode disagrees with a weak 394 cm^{-1} band reported earlier.[12b]

A weak combination band at 2669.6 cm^{-1} tracks with the stronger fundamental absorptions for PtNN and confirms the assignments. Recent thermal platinum matrix isolation experiments also observed the 2670 and 499 cm^{-1} absorptions for PtNN.[33] The former band is higher than the sum of stretching modes (2168.5 + 499.6 = 2668.1 cm^{-1}) by 1.5 cm^{-1}; this could arise from different matrix shifts for the combination and fundamentals or from a small negative anharmonicity. The

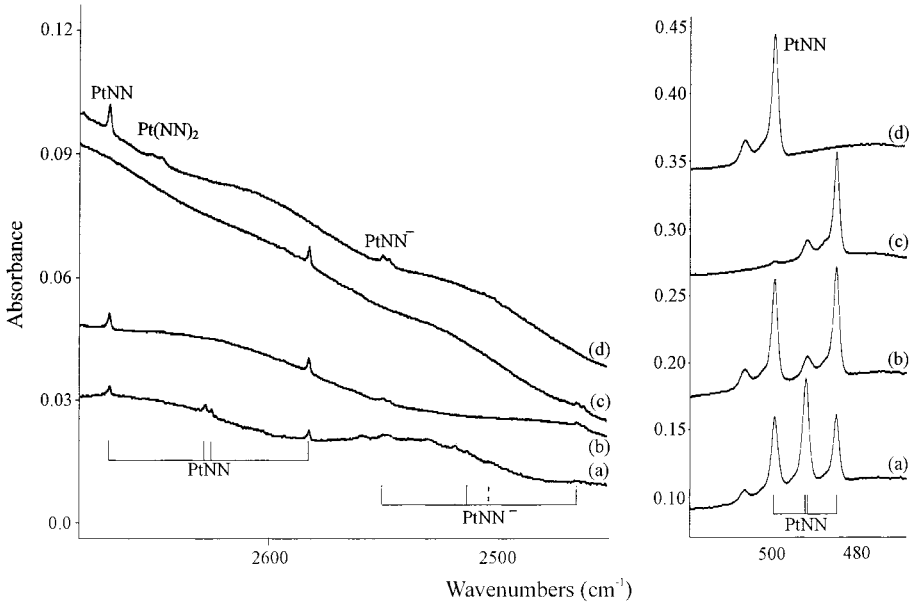

Figure 9. Infrared spectra in the 2680−2450 and 520−470 cm^{-1} regions for laser-ablated platinum co-deposited for 60 min with isotopic N_2 in argon: (a) 1% $^{14}N_2$ + 2% $^{14}N^{15}N$ + 1% $^{15}N_2$, (b) 2% $^{14}N_2$ + $^{15}N_2$, (c) 2% $^{15}N_2$, and (d) 2% $^{14}N_2$.

2669.6 cm^{-1} band is 0.4% of the fundamental band intensity, but note the clear quartet scrambled isotopic spectrum (Figure 9). For $Pt^{15}N^{15}N$, the combination band at 2582.6 cm^{-1} is also higher than the 2096.2 + 484.9 = 2581.1 cm^{-1} sum by 1.5 cm^{-1}; for $Pt^{14}N^{15}N$, the combination band at 2627.6 cm^{-1} is higher than the 2134.4 + 492.2 = 2626.6 cm^{-1} sum by 1.0 cm^{-1}, and for $Pt^{15}N^{14}N$, the combination band at 2624.9 cm^{-1} is higher than the 2131.1 + 492.2 = 2623.3 cm^{-1} sum by 1.6 cm^{-1}. The B3LYP prediction for the Pt−NN stretching mode is 15 cm^{-1} lower than the observed value, and the bending mode is 11 cm^{-1} lower than the BPW91 value. Clearly a higher level of theory is needed to describe the Pt−NN bond more accurately.

The weaker bands at 2646.6 and 2560.3 cm^{-1} with $^{14}N_2$ and $^{15}N_2$ in argon, respectively (Figures 7 and 9), track with the strong 2195.4 and 2122.2 cm^{-1} $Pt(NN)_2$ fundamentals. These bands are due to the same $\sigma_g + \sigma_u$ combination described above for $Pt(NN)_2$ in solid nitrogen. Since the σ_g (NN) fundamental is not known, no prediction of the σ_u (Pt−N) mode can be made, but these modes will be slightly lower than the nitrogen matrix values.

Similar investigations with 2% N_2 in neon gave complementary spectra, but owing to more reagent diffusion before sample solidification, the relative populations of PtNN (2169.5 cm^{-1} in neon) and $Pt(NN)_2$ (2206.9 cm^{-1} in neon) are again reversed (Figure 10). The mixed $^{14}N_2$ + $^{15}N_2$ isotopic pattern for antisymmetric and symmetric stretching modes of 15−15-Pt-14−14 at 2150 and 2238 cm^{-1}, respectively, again substantiates the linear molecule assignment. These modes are of the same symmetry, they interact, and the stronger antisymmetric mode is displaced (20 cm^{-1}) below the median of the pure isotopic antisymmetric modes, and the weaker symmetric mode gains intensity and is displaced higher by a like amount. From these displacements, a 2256 cm^{-1} estimate for the forbidden symmetric N−N stretching mode of $Pt(NN)_2$ in solid neon can be made. This is 49 cm^{-1} higher than the strong observed antisymmetric mode. Our BPW91 calculation predicts the symmetric mode higher by 49.6 cm^{-1}. The observation of virtually the same spectrum for $Pt(NN)_2$ in solid nitrogen (2205.7 cm^{-1}), argon (2195.4 cm^{-1}), and neon (2206.9 cm^{-1}) and the BPW91 prediction (2190.4 cm^{-1}) confirms this identification.

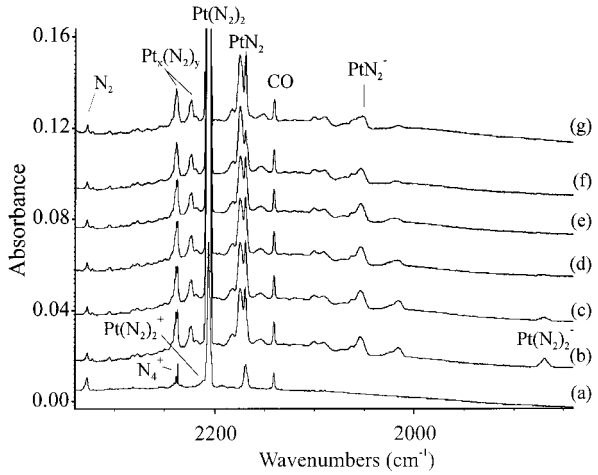

Figure 10. Infrared spectra in the 2270−1920 cm^{-1} region for laser-ablated platinum (a) co-deposited with 2% N_2 and 0.2% CCl_4 in neon for 60 min, (b) co-deposited with 2% N_2 in neon for 60 min, (c) after λ > 630 nm irradiation, (d) after λ > 470 nm irradiation, (e) after λ > 380 nm irradiation, (f) after λ > 240 nm irradiation, and (g) after 10 K annealing.

The combination band observed at 2660.0 cm^{-1} in solid neon is 9.6 cm^{-1} below the 2669.6 cm^{-1} PtNN combination band in solid argon. Since $Pt(NN)_2$ dominates PtNN (Figure 10), the $Pt(NN)_2$ assignment is more likely (a PtNN assignment would require an unlikely 9.6 cm^{-1} argon to neon red-shift in the Pt−NN fundamental). Subtracting the above 2256 cm^{-1} σ_g mode estimate from 2660 cm^{-1} gives a 404 cm^{-1} σ_u prediction, which is in excellent agreement with the deduction from the nitrogen matrix absorption and DFT calculations but not with the 360 cm^{-1} frequency reported earlier.[12b] Four combination bands are possible in the $^{14}N_2$ + $^{15}N_2$ experiment, and new bands were observed at 2683, 2634, and 2596 cm^{-1}, all much weaker than the pure isotopic 2660.0 and 2573.4 cm^{-1} features (Figure 12). Note that the mixed isotopic band profile is different for the σ_u fundamental (Figure 11) and the combination band because of the combination band selection rules. Subtraction of the two

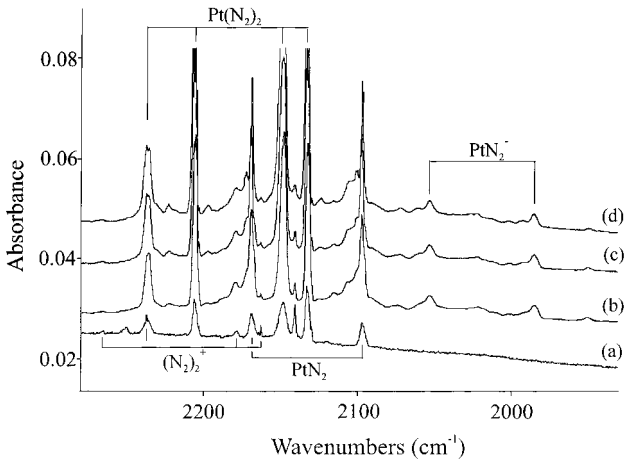

Figure 11. Infrared spectra in the 2280−1930 cm^{-1} region for laser-ablated platinum co-deposited for 60 min with $^{14}N_2 + {}^{15}N_2$ in neon at 5 K: (a) 1% $^{14}N_2$ + 1% $^{15}N_2$ + 0.2% CCl_4 in neon, (b) 0.5% $^{14}N_2$ + 0.5% $^{15}N_2$ in neon, (c) after annealing to 8 K, and (d) after annealing to 10 K.

observed Pt(14−14)(15−15) N−N stretching modes gives 446 and 396 cm^{-1} values for the two Pt−N_2 stretching modes. These differences are slightly lower than the BPW91 calculated values as found above for Pt(14−14)$_2$ and support the identification of the bis dinitrogen platinum complex. The unique character of the linear centrosymmetric molecule combination band selection rules confirms this assignment.

Pt_xNN in Argon. In experiments with 0.2%, 1%, and 2% N_2 a new 2132.3 cm^{-1} feature appeared on annealing, decreased markedly on photolysis, reappeared on higher annealing, and shifted to 2128.8 cm^{-1} on 40 K annealing (Figure 6). This feature exhibited only pure isotopic absorptions with $^{14}N_2 + {}^{15}N_2$ and two sharp intermediate components were also observed at 2095.2 and 2092.4 cm^{-1} after annealing the $^{14}N_2 + {}^{14}N^{15}N + {}^{15}N_2$ sample. These isotopic data verify the stretching mode of a single NN subunit with inequivalent atomic positions such as PtNN but 36.2 cm^{-1} lower. The first 2132.3 cm^{-1} band is assigned to PtPtNN and the annealing product to the higher Pt_x-NN complex; both of these bands are photosensitive. Green et al.[13] reached the same conclusion about the 2132 cm^{-1} annealing band in their spectra and proposed that aggregation of Pt is more favorable than aggregation of N_2, which is in agreement with our observations. BPW91 calculations predict a 4.6 cm^{-1} red-shift in the N−N stretching mode for PtPtNN relative to PtNN, which is in qualitative agreement with our observed 36.2 cm^{-1} shift.

$$Pt + N_2 \rightarrow PtNN\ (^1\Sigma^+)\ (\Delta E = -157\ kJ/mol) \quad (5)$$

$$Pt + PtNN \rightarrow PtPtNN\ (^1\Sigma)\ (\Delta E = -225\ kJ/mol) \quad (6)$$

$$N_2 + PtNN \rightarrow NNPtNN\ (\Delta E = -155\ kJ/mol) \quad (7)$$

The 2242.6, 2233.2, and 2218.2 cm^{-1} bands produced on annealing were also observed by the Argonne group.[13] Here we find a small secondary N_2 isotopic dependence and suggest that these bands are due to $Pt_x(NN)_y$ where $y = 2$ is most likely, again in accord with the more dominant diffusion of Pt than N_2. Note that the second Pt binds to PtNN more strongly than the second N_2.

Pt(NN)$_{1,2}^-$ in Solid Argon and Neon. A new 2045.8 cm^{-1} argon matrix band sharpens on annealing and decreases slightly on irradiation and more on higher annealing (Figure 6). This band was also observed using the sputtering discharge atom source[13] but not with thermal atoms.[12,33] The 2045.8 cm^{-1} feature shows no intermediate components with mixed $^{14}N_2 + {}^{15}N_2$, but weak intermediate bands are observed at 2014.3 and 2010.3 cm^{-1} with scrambled $^{14}N_2 + {}^{14}N^{15}N + {}^{15}N_2$ (Figure 8). The 2045.8 cm^{-1} absorption is due to another end-bonded dinitrogen species. Doping with 0.1% CCl_4 to capture electrons eliminated this band from the spectrum, the 2168.5 cm^{-1} PtNN band was reduced by 20%, and a new band appeared at 2230.3 cm^{-1}. In comparable 2% $^{15}N_2$ experiments with CCl_4, the 1977.6 cm^{-1} counterpart band was eliminated, the 2096.2 cm^{-1} band was reduced by 35%, and a new band appeared at 2155.7 cm^{-1}. A weaker 2550.7 cm^{-1} band decreases with the 2045.8 cm^{-1} absorption on annealing and exhibits a similar band contour. The weak 2550.7 cm^{-1} feature is tentatively assigned to the stretching mode combination band for $PtNN^-$: the difference (2550.9 − 2045.8 = 505.1 cm^{-1}) is slightly higher than the BPW91 predicted 455.2 cm^{-1} value for the Pt−N stretching mode.

The neon matrix counterpart at 2054.1 cm^{-1} exhibited analogous behavior: this band decreased slightly on photolysis and annealing, disappeared with CCl_4 added (Figure 10), and exhibited a pure isotopic doublet with $^{14}N_2 + {}^{15}N_2$ (Figure 11). The small blue shift (8.3 cm^{-1}) from argon to neon is typical: $NiCO^-$ blue shifted 13.7 cm^{-1}. The isoelectronic $PtCO^-$ species was observed at 1896.3 cm^{-1}, 169.2 cm^{-1} below PtCO in solid neon,[32] whereas $PtNN^-$ is 115.4 cm^{-1} below PtNN.

Numerous studies have shown that added CCl_4 captures most of the ablated electrons, thus reducing the yield of product anions and correspondingly increasing the yield of product cations.[29,32] These observations support assignment of the 2045.8 cm^{-1} band to $PtNN^-$ and the new 2230.3 cm^{-1} band to a nitrogen product cation in solid argon.

The $PtNN^-$ assignment receives strong support from DFT calculations. The BPW91 functional predicts a strong N−N fundamental for $PtNN^-(^2A')$ at 2028.6 cm^{-1}, 133.9 cm^{-1} below the value for PtNN, which are in excellent agreement with the experimental observations. The electron affinity implied here from the BPW91 energies (1.4 eV) is in the range for TM dihydrides.[34] On the other hand, $PtNN^+$ ($^2\Sigma^+$) is predicted to have a weak N−N fundamental at 2255.3 cm^{-1}, 92.8 cm^{-1} above PtNN, which is not observed here.

Additional charged species are observed in solid neon. The sharp 2237.4 cm^{-1} feature is enhanced by CCl_4 and is independent of metal. This band is in excellent agreement with the $(NN)_2^+$ absorption in solid neon produced by discharge excitation,[35] which means that energy in excess of 15.6 eV, the ionization energy of N_2,[36] is available in the laser plume to produce N_2^+ in these experiments for reaction with N_2 to form $(NN)_2^+$. An analogous conclusion was reached about the formation of CO^+.[29] The sharp 1648.7 cm^{-1} band is between the solid nitrogen (1657.7 cm^{-1}) and gas phase (1644.7 cm^{-1}) fundamentals for N_3 radical[16,24,37] and is assigned accordingly.

The weaker 1869.0 cm^{-1} neon matrix band is even more photosensitive, i.e., substantial reduction by $\lambda > 630$ nm radiation, and is eliminated by CCl_4 (Figure 10). The crucial mixed isotopic evidence is shown in Figure 12: this feature matches the mixed isotopic spectrum for Pt(NN)$_2$. The intermediate mixed antisymmetric stretching mode isotopic component at 1833 cm^{-1} is below the median of pure isotopic values (1839.5 cm^{-1}), and the weaker symmetric counterpart is observed at 1903 cm^{-1}. Our BPW91 calculations find a linear, centrosymmetric $Pt(NN)_2^-$ anion 78 kJ/mol more stable than Pt(NN)$_2$ and predict a very strong (2469 km/mol) antisymmetric

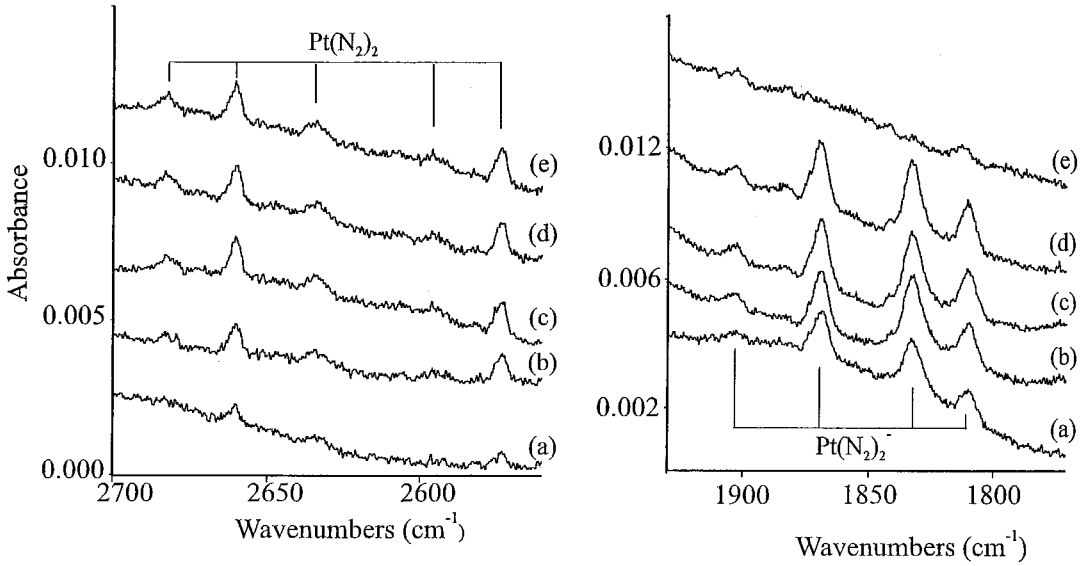

Figure 12. Infrared spectra in the 2700−2560 and 1930−1770 cm^{-1} regions for laser-ablated platinum co-deposited with 2% $^{14}N_2$ + 2% $^{15}N_2$ in neon at 5 K: (a) after 30 min deposition, (b) after 60 min deposition, (c) after 80 min deposition, (d) after 8 K annealing, and (e) after $\lambda > 240$ nm irradiation.

TABLE 6: Experimental and Theoretical Frequencies (cm^{-1}) for Mononitrides of the Third-Row Transition Metals

medium	LaN	HfN	TaN	WN	ReN	OsN	IrN	PtN
gas phase[a]		923.9			1121.9	1137.0	1113.6	937.0
argon[b]			1063.0	1059.5	1121.4	1130.3	1004.5	927.9
nitrogen[b]	761.7	883.4	962.9	1027.9	1083.8	1049.6	1002.3	893.1
DFT (BPW91)	786.6	950.6	1099.7	1080.7	1164.7	1219.1	1198.6	975.2
[state]	$[^1\Sigma^+]$	$[^2\Sigma^+]$	$[^1\Sigma^+]$	$[^4\Sigma^-]$	$[^3\Sigma^-]$	$[^2\Delta]$	$[^1\Sigma^+]$	$[^2\Pi]$
			1037.0					
			$[^3\Delta]$[c]					

[a] References given in matrix reports, refs 3, 4, 6, 7, and ref 8. [b] References 2−7, this work. [c] The singlet and triplet states are within 1 kJ/mol.

N−N stretching mode at 1928.4 cm^{-1}, in excellent agreement with the observed frequency. Considering that this is a platinum complex species and an anion, this agreement is even more remarkable. We note that the antisymmetric C−O mode of $Pt(CO)_2^-$ observed at 1844.0 cm^{-1} has a high calculated infrared intensity (2898 km/mol) and is below the fundamental for $PtCO^-$ observed at 1896.3 cm^{-1} (infrared intensity 1132 km/mol).[32]

What is the possibility of detecting $Pt(NN)_{1,2}^+$ cations, which are surely made in these experiments? Recall that $Pt(CO)_{1,2,3}^+$ cations were observed in similar carbonyl experiments. However, the latter cations have calculated infrared intensities of 321, 744, and 1140 km/mol,[32] and the $Pt(NN)_{1,2}^+$ cations have calculated infrared intensities of only 21 and 78 km/mol (Table 4). The $Pt(NN)_2^+$ cation is tentatively identified at 2210.0 cm^{-1} in solid nitrogen. A weak 2212.1 cm^{-1} band observed with CCl_4 doping (Figure 10a) increases slightly on 8 K annealing and disappears on UV/Vis irradiation. Unfortunately, the $^{15}N_2$ region is masked by other absorptions. This weak band is tentatively assigned to $Pt(NN)_2^+$.

Third-Row Mononitrides. Almost all of the third-row transition metal nitrides MN have been observed in argon or nitrogen matrices, and gas-phase data are available in most cases. The only exception is AuN, which has not been observed.[38] Calculations at the BPW91 level for AuN predict the molecule to be an extremely weak infrared absorber (1 km/mol) at 575.7 cm^{-1} for the $^3\Sigma^-$ ground state, and it is likely that the molecule was made but could not be detected.

As shown in Table 6, the overall trend in frequencies is a steady increase from the start of the row, reaching a maximum at ReN and OsN, and then a decrease at the far right, ending at PtN. This is probably due to the increasing electron count across the series which initially strengthens the bond by filling bonding orbitals but eventually weakens it as antibonding orbitals become occupied.

In most cases MN absorptions in both argon and pure nitrogen are observed. The former is due to isolated MN, whereas the latter is probably complexed by additional N_2 ligands and/or interacts more strongly with the nitrogen matrix. This complexation can cause a significant red-shift in the absorption frequency: a good example is OsN, which absorbs ~80 cm^{-1} lower in a pure nitrogen matrix than in argon.[6] In other cases, the red-shift is far smaller and there is no obvious correlation between the size of this shift and the position of the metal in the periodic table. Gas phase absorption frequencies are commonly very close to the argon matrix values; the ReN comparison is a good case in point.[3]

DFT calculations for these molecules are commonly very useful, although direct comparisons between calculated frequencies and nitrogen matrix values are complicated by the red-shift discussed above. The MN frequencies calculated using the BPW91 functional are consistently high by several tens of wavenumbers and are a useful tool in assigning spectra. For example, they indicate that the singlet state of TaN is the correct ground state since the frequency for this state is high by 36.7 cm^{-1}, whereas the calculated triplet frequency is below the observed values.

Conclusions

Platinum atoms have been reacted with pure nitrogen to produce several new metal nitrides. The platinum products are

dominated by PtN and species derived from PtN including NNPtN, Pt_2N, PtNNPt, and Pt_x−PtN. The azide PtNNN increases on annealing from the reaction of Pt with N_3 radical. The NNPtN isomer is more photosensitive than PtNNN.

New information is obtained for $Pt(NN)_x$ complexes: (a) the important Pt−NN stretching mode has been observed at 499.6 cm^{-1} for PtNN along with the strong N−N stretching mode and their combination band, (b) mixed isotopic data in the strong fundamental and combination band confirm the identification of linear $Pt(NN)_2$, and (c) the earlier identification of $Pt(NN)_3$ must be rejected. The N−N fundamental for PtNN in solid neon at 2169 cm^{-1} is lower than the fundamental for chemisorbed N_2 at Pt(111) defect sites (2222 and 2234 cm^{-1}):[39−41] it appears that the N_2 interaction with a single naked Pt atom is stronger. However, we note absorptions in the 2220−2260 cm^{-1} region for higher metal cluster $Pt_x(NN)_y$ species.

Complementary neon matrix investigations facilitate identification of the charged species $PtNN^-$ and $Pt(NN)_2^-$: the latter is photosensitive to red light. The N−N fundamental is 115 cm^{-1} lower in $PtNN^-$ than in PtNN, which is in accord with alkali promotion of N_2 dissociation.[42] In addition, the $(NN)_2^+$ cation is observed in agreement with previous work.[35]

DFT using the LANL2DZ pseudopotential reproduces the experimental results better for nitrogen complexes than for platinum nitrides; the calculated frequencies are consistently too high by several tens of wavenumbers using the BPW91 functional. Higher level calculations on PtNN are warranted.[43]

The results for PtN are compared with those for the other mononitrides of the third-row transition metals and are found to complete the trend in frequencies.

Acknowledgment. We gratefully acknowledge support from N.S.F. Grants CHE 97-00116 and CHE 00-78836, assistance of G. V. Chertihin, and helpful correspondence with L. Manceron.

References and Notes

(1) Somorjai, G. A. *Introduction to Surface Chemistry and Catalysis*; John Wiley and Sons: New York, 1994.
(2) Chertihin, G. V.; Bare, W. D.; Andrews, L. *J. Phys. Chem. A* **1998**, *102*, 3697 (La + N_2).
(3) Zhou, M. F.; Andrews, L. *J. Phys. Chem. A* **1998**, *102*, 9061 (Ta, Re + N_2).
(4) Kushto, G. P.; Souter, P. F.; Chertihin, G. V.; Andrews, L. *J. Chem. Phys.* **1999**, *110*, 9020 (Hf + N_2).
(5) Andrews, L.; Souter, P. F.; Bare, W. D.; Liang, B. *J. Phys. Chem. A* **1999**, *103*, 4649 (W + N_2).
(6) Citra, A.; Andrews, L. *J. Phys. Chem. A* **2000**, *104*, 1152 (Os + N_2).
(7) Friedman-Hill, E. J.; Field, R. W. *J. Chem. Phys.* **1994**, *100*, 6141.
(8) (a) Chi, Q.; Musaev, D. G.; Morokuma, K. *J. Chem. Phys.* **1998**, *108*, 8418. (b) Andrews, L.; Wang, X.; Manceron, L. *J. Chem. Phys.* **2001**, *114*, 1559.
(9) Jung, K. Y.; Steimle, T. C.; Dai, D.; Balasubramanian, K. *J. Chem. Phys.* **1995**, *102*, 643.
(10) Dai, D.; Balasubramanian, K. *J. Mol. Spectrosc.* **1995**, *172*, 421.
(11) Burdett, J. K.; Graham, M. A.; Turner, J. J. *J. Chem. Soc., Dalton Trans. I* **1972**, 1620 (M + N_2)
(12) (a) Kundig, E. P.; Moskovits, M.; Ozin, G. A.; *Can. J. Chem.* **1973**, *51*, 2710 (Pt + N_2). (b) Klotzbücher, W.; Ozin, G. A. *J. Am. Chem. Soc.* **1975**, *97*, 2672 (M + N_2).
(13) Green, D. W.; Thomas, G. J.; Gruen, D. M. *J. Chem. Phys.* **1973**, *58*, 5453 (Pt + N_2).
(14) Manceron, L.; Alikhani, M. E.; Joly, H. A. *Chem. Phys.* **1998**, *228*, 73 (Ni + N_2).
(15) Burkholder, T. R.; Andrews, L. *J. Chem. Phys.* **1991**, *95*, 8697.
(16) Hassanzadeh, P.; Andrews, L. *J. Phys. Chem. A* **1992**, *96*, 9177.
(17) Frisch, M. J.; Trucks, G. W.; Schlegel, H. B.; Gill, P. M. W.; Johnson, B. G.; Robb, M. A.; Cheeseman, J. R.; Keith, T.; Petersson, G. A.; Montgomery, J. A.; Raghavachari, K.; Al-Laham, M. A.; Zakrzewski, V. G.; Ortiz, J. V.; Foresman, J. B.; Cioslowski, J.; Stefanov, B. B.; Nanayakkara, A.; Challacombe, M.; Peng, C. Y.; Ayala, P. Y.; Chen, W.; Wong, M. W.; Andres, J. L.; Replogle, E. S.; Gomperts, R.; Martin, R. L.; Fox, D. J.; Binkley, J. S.; Defrees, D. J.; Baker, J.; Stewart, J. P.; Head-Gordon, M.; Gonzalez, C.; Pople, J. A. *Gaussian 94*, revision B.1; Gaussian, Inc.: Pittsburgh, PA, 1995.
(18) Becke, A. D. *Phys. Rev. A* **1988**, *38*, 3098.
(19) Perdew, J. P.; Wang, Y. *Phys. Rev. B* **1992**, *45*, 13244.
(20) Becke, A. D. *J. Chem. Phys.* **1993**, *98*, 5648.
(21) Krishnan, R.; Binkley, J. S.; Seeger, R.; Pople, J. A. *J. Chem. Phys.* **1980**, *72*, 650.
(22) Wadt, W. R.; Hay, P. J. *J. Chem. Phys.* **1985**, *82*, 284.
(23) Hay, P. J.; Wadt, W. R. *J. Chem. Phys.* **1985**, *82*, 299.
(24) Tian, R.; Facelli, J. C.; Michl, J. *J. Phys. Chem.* **1988**, *92*, 4073.
(25) Zhou, M. F.; Andrews, L. *J. Phys. Chem. A* **2000**, *104*, 1648 (Ga + N_2).
(26) Andrews, L.; Zhou, M. F.; Chertihin, G. V.; Bare, W. D.; Hannachi, Y. *J. Phys. Chem. A* **2000**, *104*, 1656 (Al + N_2).
(27) Citra, A.; Andrews, L. *J. Phys. Chem. A* **1999**, *103*, 3410 (Rh + N_2).
(28) Zhou, M. F.; Andrews, L. *J. Am. Chem. Soc.* **1999**, *121*, 9171.
(29) Zhou, M. F.; Andrews, L. *J. Phys. Chem. A* **1999**, *103*, 7773 (Rh + CO).
(30) Darling, J. R.; Ogden, J. S. *J. Chem. Soc., Dalton Trans.* **1972**, 2496.
(31) Bytheway, I.; Wong, M. W. *Chem. Phys. Lett.* **1998**, *282*, 219.
(32) Liang, B.; Zhou, M. F.; Andrews, L. *J. Phys. Chem. A* **2000**, *104*, 3905 (Pt + CO).
(33) Manceron, L., unpublished results (Pt + N_2).
(34) Miller, A. E. S.; Feigerle, C. S.; Lineberger, W. C. *J. Chem. Phys.* **1986**, *84*, 4127.
(35) Thompson, W. E.; Jacox, M. E. *J. Chem. Phys.* **1990**, *93*, 3856.
(36) Ogawa, M.; Tanaka, Y. *Can. J. Phys.* **1962**, *40*, 1593.
(37) Brazier, C. R.; Bernath, P. F.; Burkholder, J. B.; Howard, C. J., Jr. *J. Chem. Phys.* **1988**, *89*, 1762.
(38) Citra, A.; Andrews, L., unpublished results, 1999 (Au + N_2).
(39) Arumainayagam, C. R.; Tripa, C. E.; Xu, J.; Yates, J. T., Jr. *Surf. Sci.* **1996**, *360*, 121.
(40) Tripa, C. E.; Zubkov, T. S.; Yates, J. T., Jr.; Mavrikakis, M.; Nϕrskov, J. K. *J. Chem. Phys.* **1999**, *111*, 8651.
(41) Zehr, R.; Solodukhin, A.; Hayne, B. C.; French, C.; Harrison, I. *J. Phys. Chem. B* **2000**, *104*, 3094.
(42) Mortensen, J. J.; Hammer, B.; Nørskov, J. K. *Phys. Rev. Lett.* **1998**, *80*, 4333.
(43) A very early calculation for PtNN reports a 2508 cm^{-1} frequency at the HONDO6 level: Basch, H. *Chem. Phys. Lett.* **1985**, *116*, 58.